Cell Metabolism, Volume *23*

Supplemental Information

VEGFB/VEGFR1-Induced Expansion of Adipose Vasculature Counteracts Obesity and Related Metabolic Complications

Marius R. Robciuc, Riikka Kivelä, Ian M. Williams, Jan Freark de Boer, Theo H. van Dijk, Harri Elamaa, Feven Tigistu-Sahle, Dmitry Molotkov, Veli-Matti Leppänen, Reijo Käkelä, Lauri Eklund, David H. Wasserman, Albert K. Groen, and Kari Alitalo

Table S1. Body composition analysis by DEXA of AAV transduced mice, related to Figure 1*

	Standard diet			High fat diet		
	AAV-Ctrl (7)	AAV-B186 (7)	p value	AAV-Ctrl (7)	AAV-B186 (8)	p value
BW (g)	28,5	27,9	0,55	50,2	50,8	0,69
BMD	0,051	0,049	0,63	0,049	0,048	0,28
BMC	0,37	0,37	0,98	0,44	0,44	0,91
Area	7,39	7,53	0,55	8,86	9,23	0,21
Lean (g)	23,8	24,2	0,77	26,6	27,7	0,41
Fat (g)	4,11	3,57	0,31	20,8	20,5	0,71
Fat %	14,8	12,8	0,29	43,8	42,5	0,52

* Data is presented as mean group value; p value was calculated by using two-tailed unpaired t-test.
BMD, bone mineral density; BMC, bone mineral content

Table S2. Biometrical and clinical chemistry analysis after 14 weeks of HFD, related to Figure 1*

	AAV-Ctrl (n=10)	AAV-B186 (n=11)	p value
Body weight (g)	46,4 ± 1.1	46,1 ± 0.9	0,835
Heart mass (g)	0.14 ± 0.01	0.18 ± 0.01	< 0.001
Liver mass (g)	2.10 ± 0.3	2.13 ± 0.2	0,879
eWAT mass (g)	1,79 ± 0.2	2,31 ± 0.1	0,047
iWAT mass (g)	2.29 ± 0.2	2.16 ± 0.1	0,405
BAT mass (g)	0,82 ± 0.1	0,88 ± 0.1	0,405
$VEGFB_{186}$ (ng/ml)	n.d.	23,4 ± 2.9	-
s-CHOL (mM)	8,1 ± 0.8	8,4 ± 0.3	0,405
s-TGs (mM)	0,34 ± 0.1	0,28 ± 0.1	0,013
f-Glucose (mM)	10,9 ± 1,2	9,8 ± 0,3	0,044
f-Insulin (ng/ml)	3,33 ± 0.1	1,57 ± 0.2	0,013
NEFA (mM)	1,08 ± 0.1	0,89 ± 0.1	0,128

* Data is presented as mean ± SEM; p value was calculated by using two-tailed unpaired t-test

Table S3. Body composition analysis by DEXA of Flt1-flox and Flt1-EC^{KO} mice transduced with AAV, related to Figure 5*

	Flt1-flox; AAV-Ctrl (8)	Flt1-EC^{KO}; AAV-B186 (8)	p value
BW (g)	34,5	30,9	0,01
BMD	0,05	0,05	0,38
BMC	0,36	0,36	0,78
Area	7,05	7,17	0,70
Lean (g)	21,7	23,1	0,01
Fat (g)	11,3	6,5	0,00
Fat %	34,1	21,8	0,00

* Data is presented as mean group value; p value was calculated by using two-tailed unpaired t-test.
BMD, bone mineral density; BMC, bone mineral content

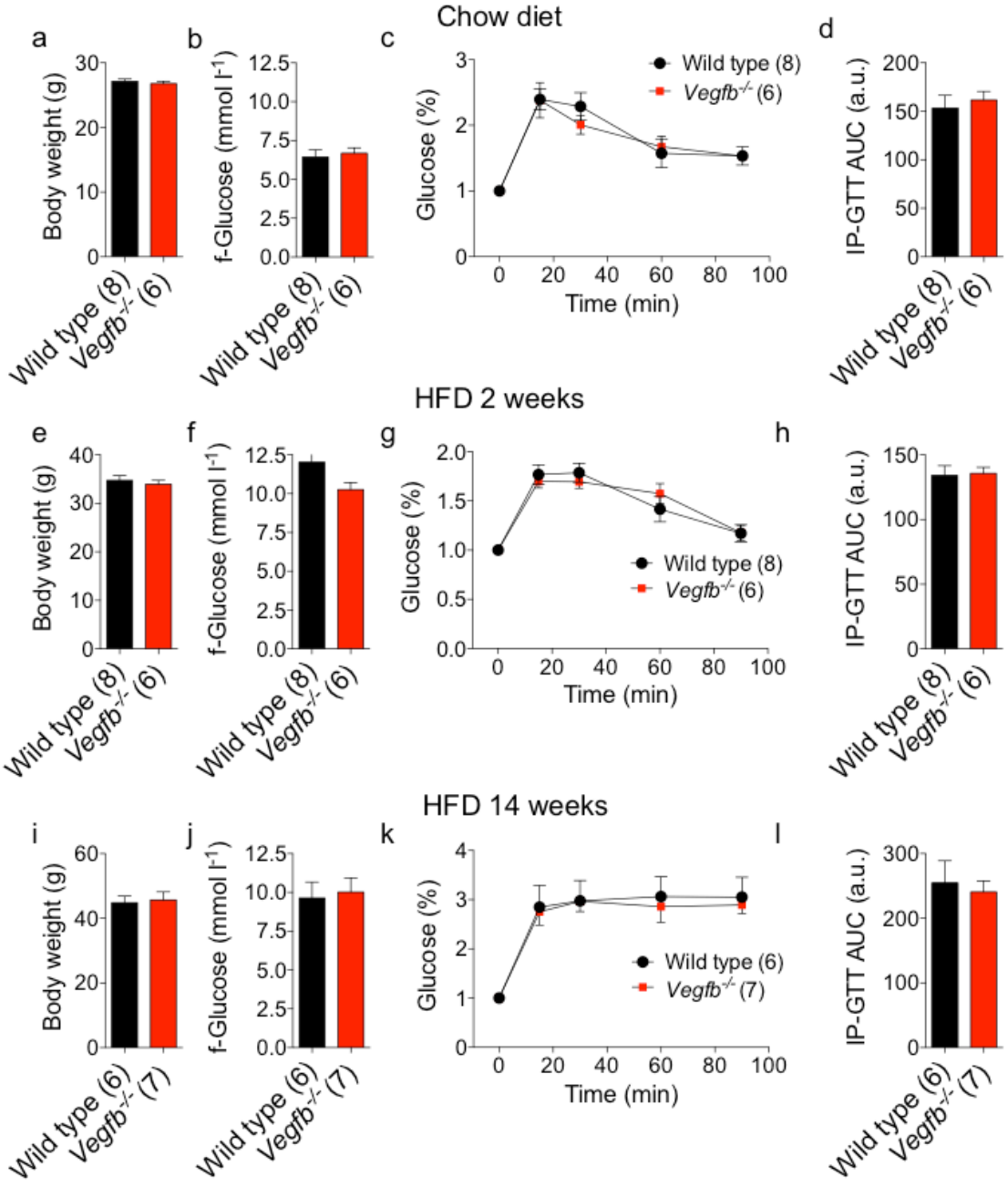

Figure S1. No difference in body weight or glucose tolerance between HFD fed *Vegfb -/-* and WT mice, related to Figure 1. Body weight, fasting glucose, IP-GTT and AUC analysis were performed in C57Bl/6J male mice fed standard diet (a, b c and d, respectively), 2 weeks of HFD (e, f, g and h, respectively) or 14 weeks of HFD (i, j, k and l, respectively). WT control mice (a-h) were obtained from parallel WT matings or (i-l) from littermate controls from *Vegfb* +/- x *Vegfb* +/- matings.

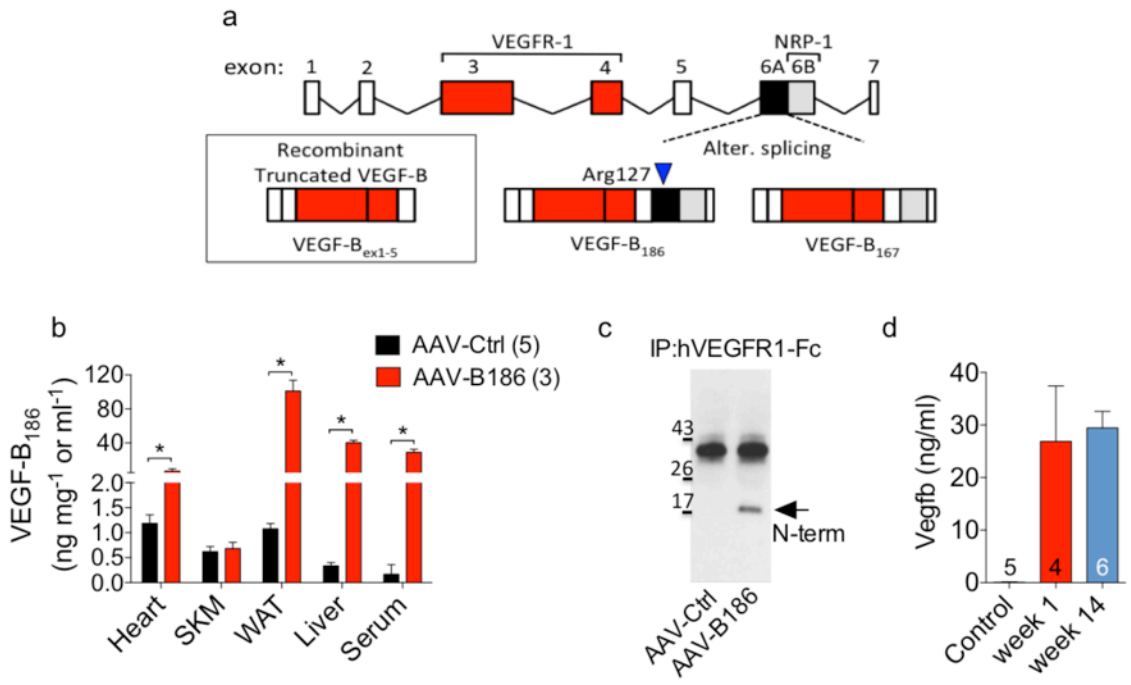

Figure S2. Schematic representation of the VEGFB isoforms and validation of AAV-B186 transduction efficiency *in vivo*, related to Figure 1. (a) Schematic representation of *Vegfb* gene and the isoforms employed in this study. The wild type isoforms $VEGFB_{186}$ and $VEGFB_{167}$ bind to both VEGFR1 and NRP-1 whereas the recombinant isoform $VEGFB_{ex1-5}$ bind only to VEGFR1. VEGFR1 binding site are in exons 3-4, highlighted in red. (b) $VEGFB_{186}$ protein levels in tissues and serum measured by a $VEGF_{186}$ specific ELISA based on capture antibody AF590 (R&D Systems) and detection antibody BAF767 (R&D Systems). (c) $VEGFB_{186}$ precipitation from mouse serum using hVEGFR1-Fc. VEGFB was detected by using the antibody AF590 (R&D Systems) against the VEGFB N-terminal part (Pro22-Ala107) in western blotting. (d) VEGFB186 concentration in sera was measured by ELISA at the indicated timepoints after transduction with AAV-B186. Number of mice is indicated in the figure. Data are represented as mean ± SEM. * $p < 0.05$, calculated by using the two-tailed unpaired t test.

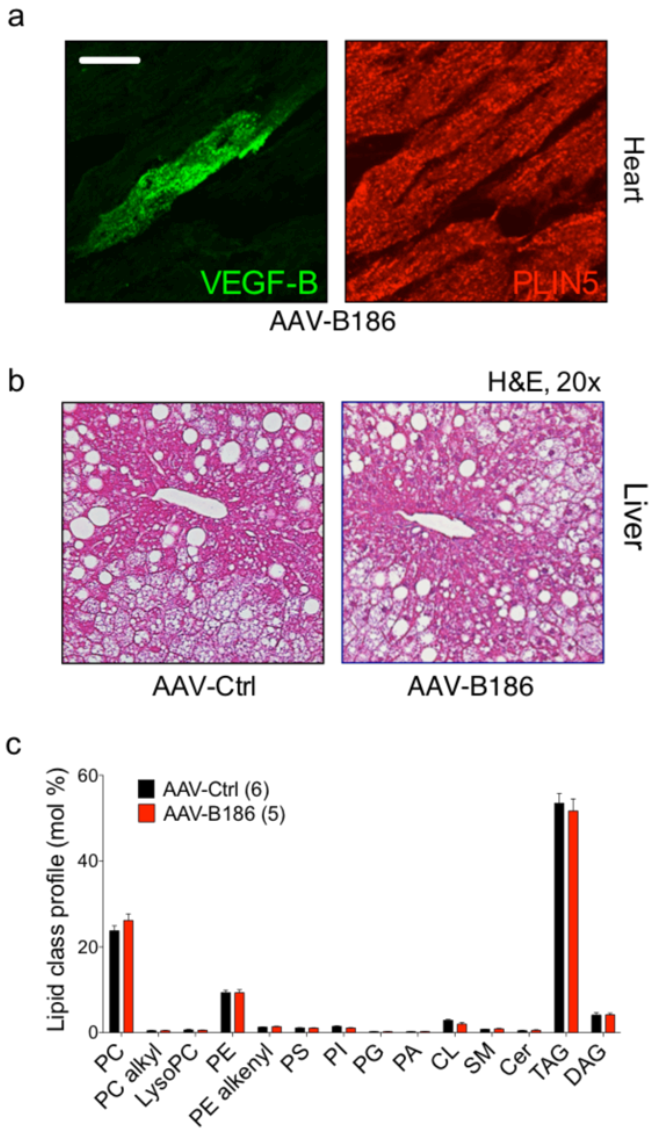

Figure S3. Similar ectopic lipid deposition in HFD fed AAV-Ctrl and AAV-B186 mice, related to Figure 1. Samples were analyzed from C57Bl/6JOlaHsd male mice transduced with the indicated AAVs and fed HFD for 14 weeks. (a) Comparison of lipid droplet content (PLIN5) in transduced and non-transduced cardiac muscle fibers. (b) Haematoxylin-eosin stained paraffin sections from the liver. (c) Lipid class profiles in the liver analyzed by mass spectrometry. Scale bar: 25 µm. Number of mice is indicated in the figure. Data are represented as mean ± SEM.

PC, phosphatidylcholine diacyl species; PC alkyl, phosphatidylcholine alkyl-acyl species; LysoPC, lysophosphatidylcholine; PE, phosphatidylethanolamine diacyl species; PE alkenyl, phosphatidylethanolamine alkenyl-acyl species; PS, phosphatidylserine; PI, phosphatidylinositol; PG, phosphatidylglycerol; PA, phosphatidic acid; CL, cardiolipin; SM, sphingomyelin; Cer, ceramide; TAG, triacylglycerol; DAG diacylglycerol.

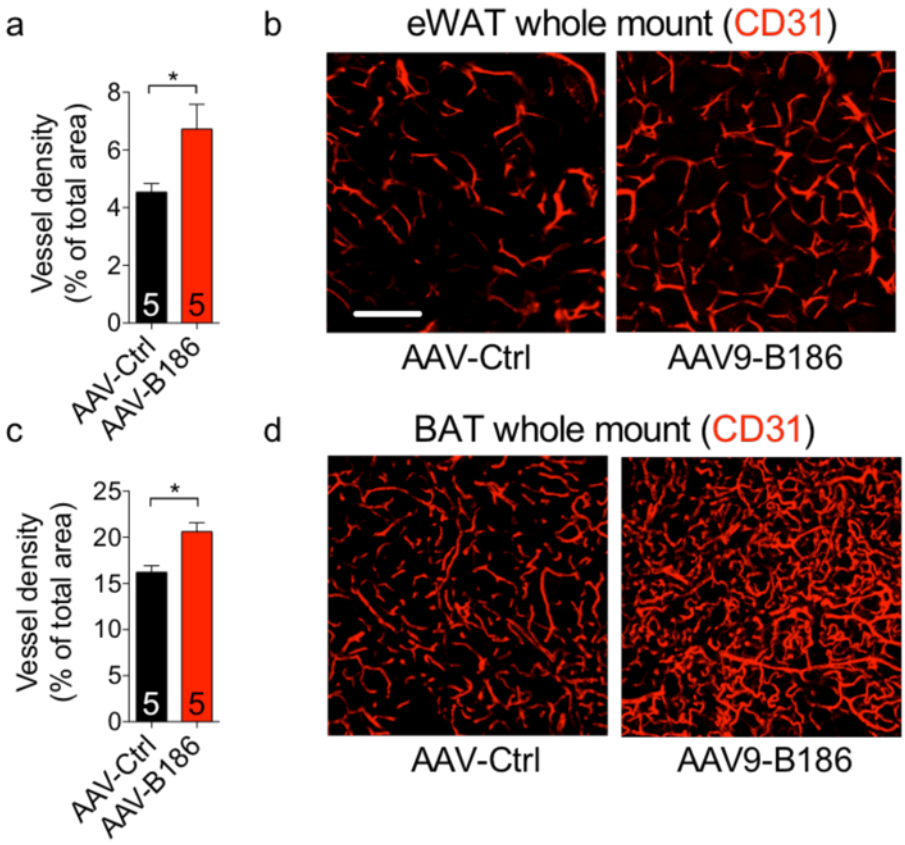

Figure S4. Expansion of microvasculature network in adipose tissues from AAV-B186 mice fed HFD for six (a, b) or 14 weeks (c, d) , related to Figure 1. Blood vessel area quantification and representative confocal projections from eWAT (a, b) and BAT (c, d), stained for CD31. eWAT vasculature analysis was performed in mice fed HFD for only six week because longer HFD feeding induced very strong inflammation in the control group, which interfered with the analysis. Number of mice is indicated in the figure. Data are represented as mean ± SEM. Scale bar: 100 μm * $p < 0.05$, calculated by using the two-tailed unpaired t test.

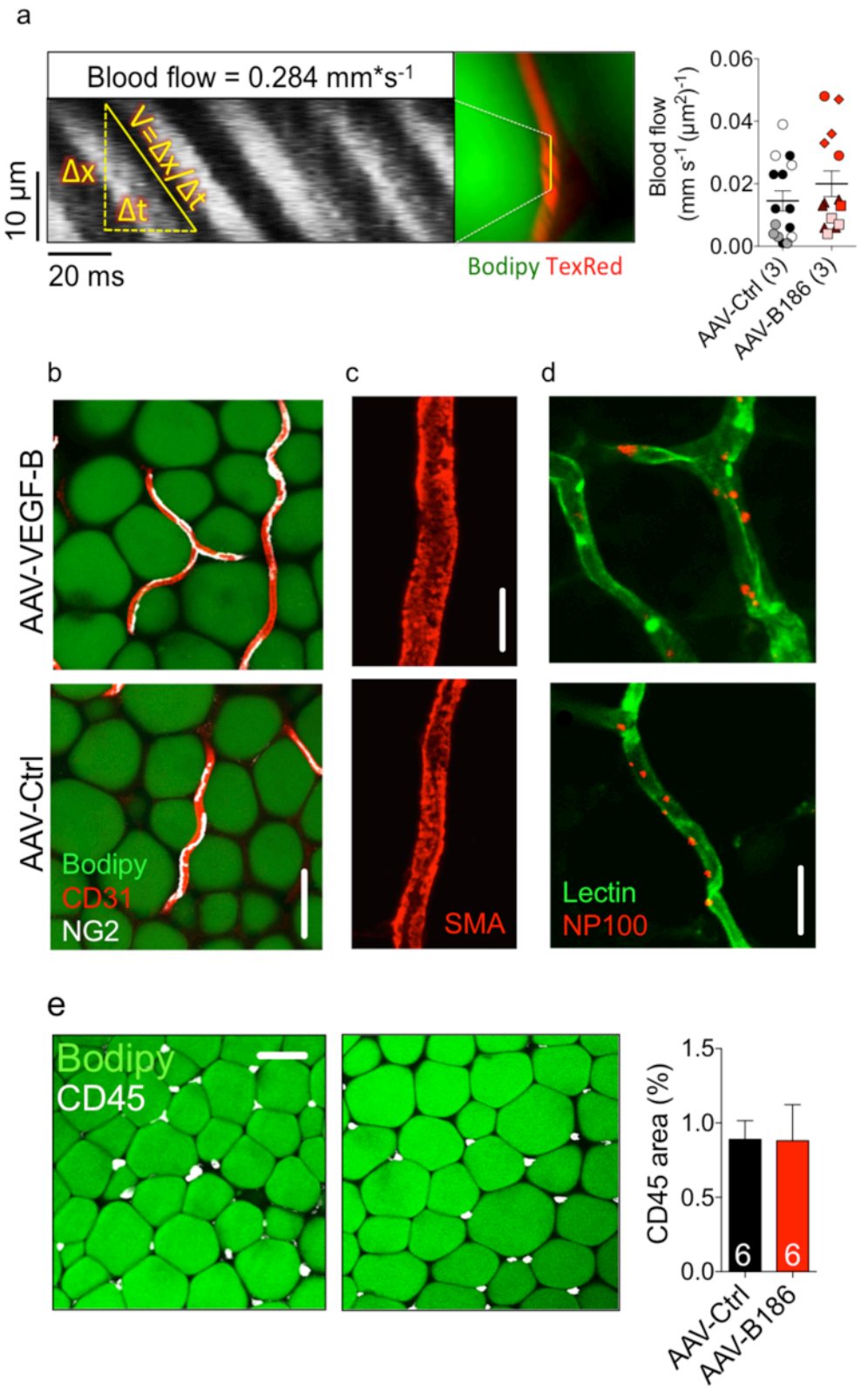

Figure legend on the next page

Figure S5. Normal blood flow and structure of microvasculature, and absence of leucocyte infiltration in adipose tissue of VEGFB transduced mice, related to Figure 2. C57Bl/6JOlaHsd male mice were transduced for with the indicated AAVs. (a) Representative image of intravital two-photon microscopy showing repeated line scans from lumen of eWAT capillaries and quantification of blood flow speed. Each point of the graph represents the blood flow speed normalized to crossectional area from one capillary (mm s^{-1} $(\mu m^2)^{-1}$). Confocal projections of adipose tissue whole mount staining for (b) CD31 and NG2 (pericytes) or (c) SMA (smooth muscle cells). (d) Optical sections from whole mounts of adipose tissue perfused with Lectin and 100 nm nanoparticles (NP100) indicate that capillaries in the VEGFB transduced mice adipose tissue are not leaky. (e) Representative optical sections and quantification of CD45 area in eWAT. Adipocytes were stained with Bodipy (green). Number of mice is indicated in the figure. Scale bar 50 μm in a and e; 25 μm in b and c.

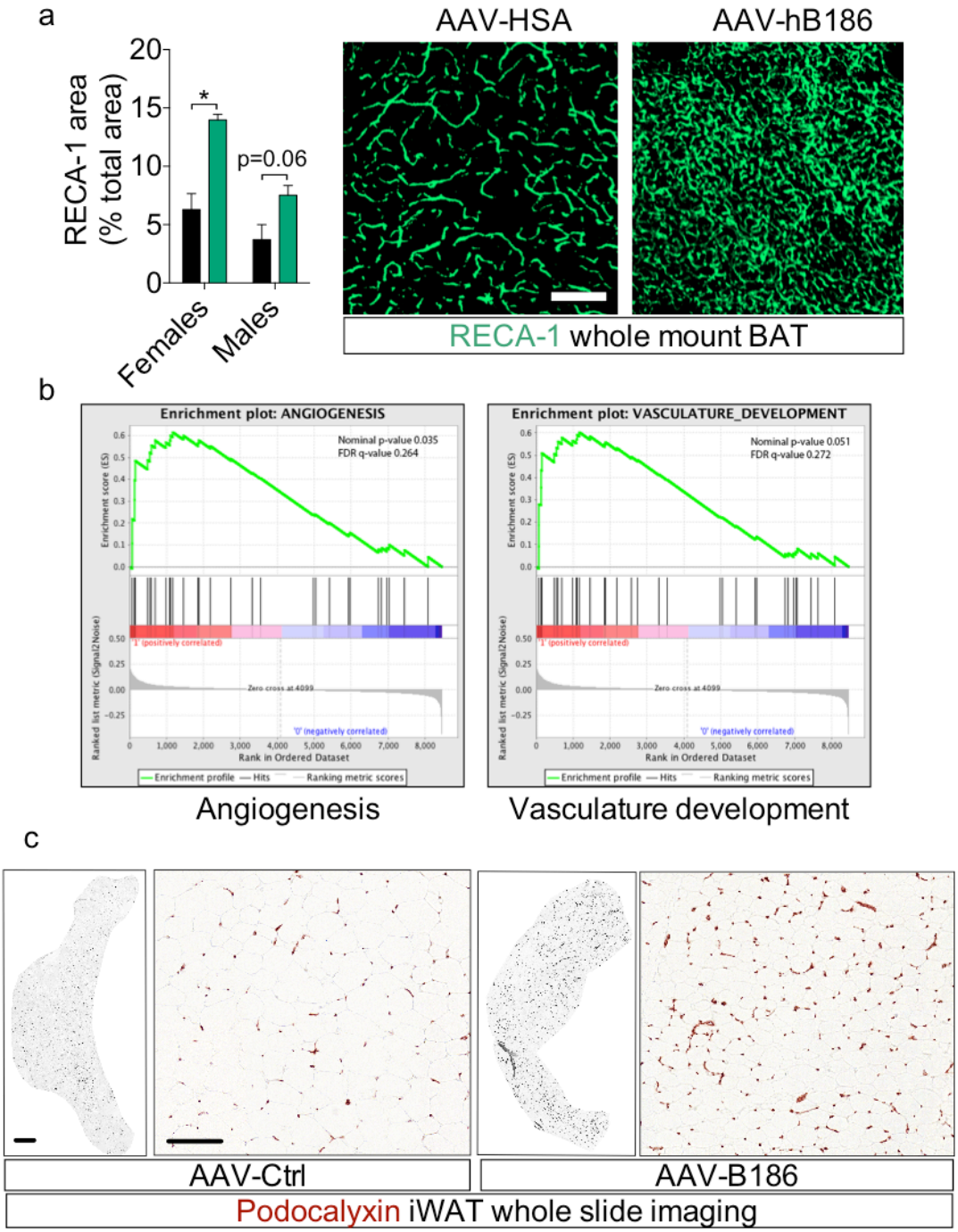

Figure legend on next page

Figure S6. VEGFB induced angiogenesis in rat brown adipose tissue (BAT) and female mouse inguinal WAT (iWAT), related to Figure 2. AAVs encoding human serum albumin (AAV-HSA) or human VEGFB (AAV-hB186) were injected via the tail vein into rats, in a and b. Mouse females were transduced with the indicated AAVs, in c. The animals were fed a standard diet. (a) Vessel area quantification and representative confocal projections from whole mount BAT preparations stained for the endothelial marker RECA-1 four weeks after gene transduction, n = 3 rats per groups (b) Pathway analysis of RNA microarray data from BAT showing enrichment of mRNA levels of genes involved in angiogenesis and vasculature development. (c) iWAT vasculature was stained for Podocalyxin and imaged using 3DHISTECH Pannoramic 250 FLASH II digital slide scanner. Representative whole slide and zoomed in images are shown. Scale bar 100 μm, in a and for zoomed images in panel c; 2 mm for whole slide image in panel c. Data are represented as mean ± SEM. * $p < 0.05$, calculated with two-tailed unpaired t-test.

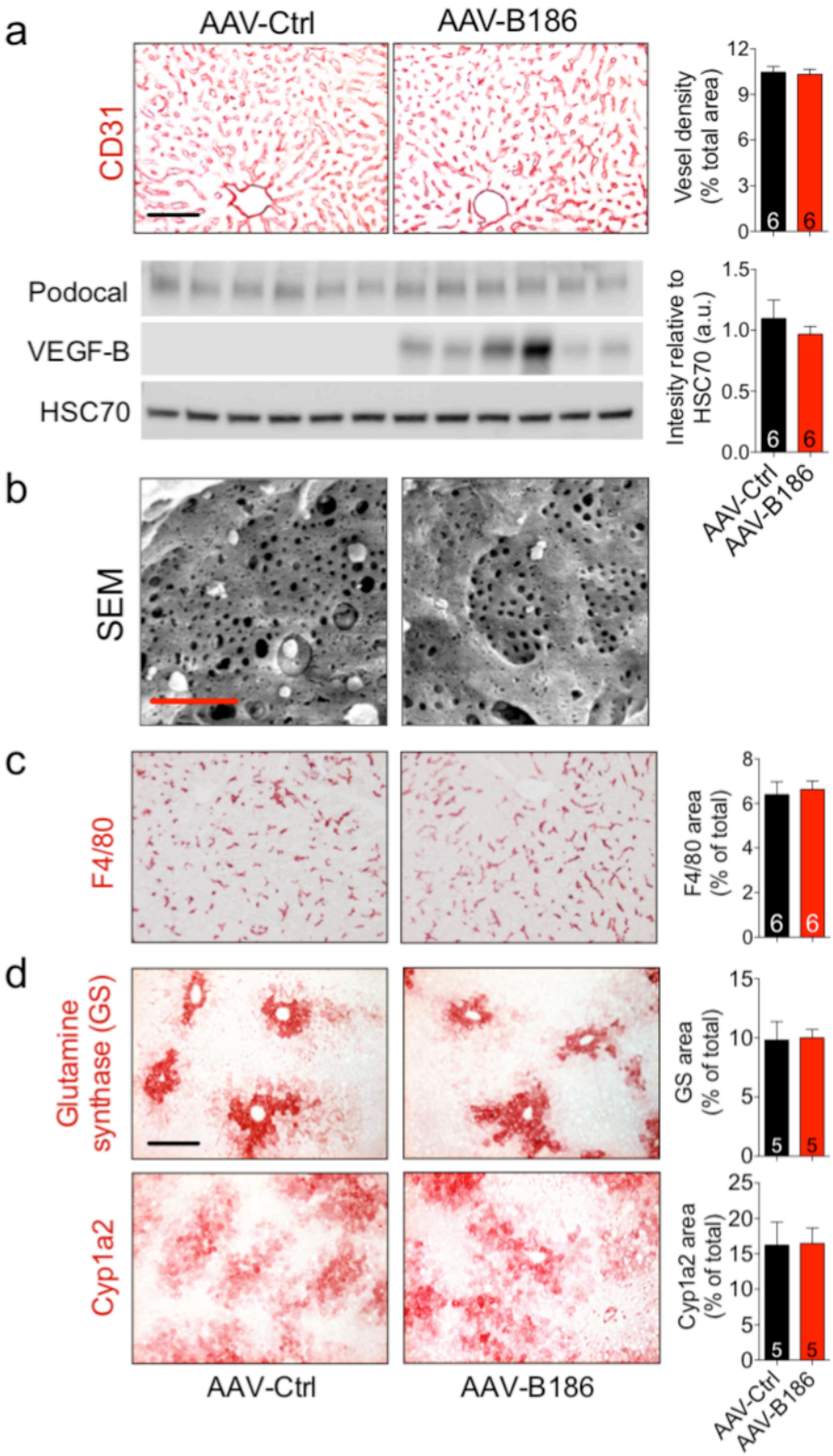

Figure legend on next page

Figure S7. VEGFB has no effect on liver microvasculature or zonation, related to Figure 1 and 2. (a) IHC of liver sinusoids and Western blot analysis of endothelial cell marker Podocalyxin. (b) Scanning electron microscopy images of the liver sinusoidal endothelial cell fenestri. IHC analysis of (c) Kupfer cells (F4/80 staining) and (d) liver zonation using two markers, glutamine synthase and Cyp1a2. Number of mice is indicated in the figure. Data are represented as mean ± SEM. Scale bars: 100μm in a, 1μm in b, 200μm in c.

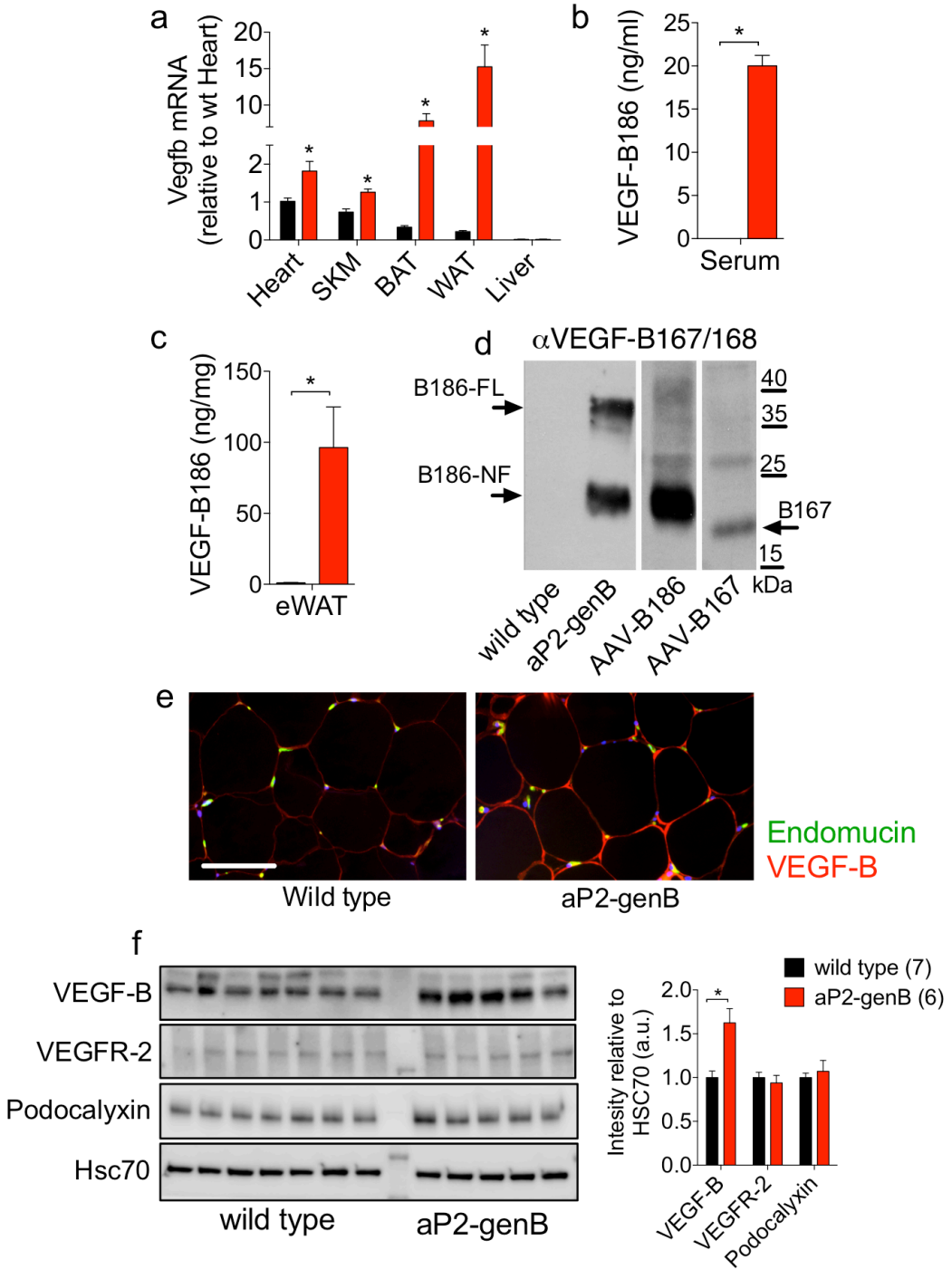

Figure legend on next page

Figure S8. Validation of the aP2-genB mouse model, related to Figure 2. (a) Comparison of Vegfb mRNA expression levels in various tissues by real time PCR. (b) $VEGFB_{186}$ protein in serum and (c) eWAT measured by ELISA. (d) Western blotting of eWAT, showing that VEGFB186 is the main isoform. (e) Endomucin and VEGFB immunofluorescence staining of paraffin sections from eWAT, scale bar 50 μm. (f) Western blot images and quantification of protein expression are shown. N = 5-7 mice/group. Data are represented as mean ± SEM. * $p < 0.05$, calculated by using the two-tailed unpaired t-test. FL, full length, NF, N-terminal fragment.

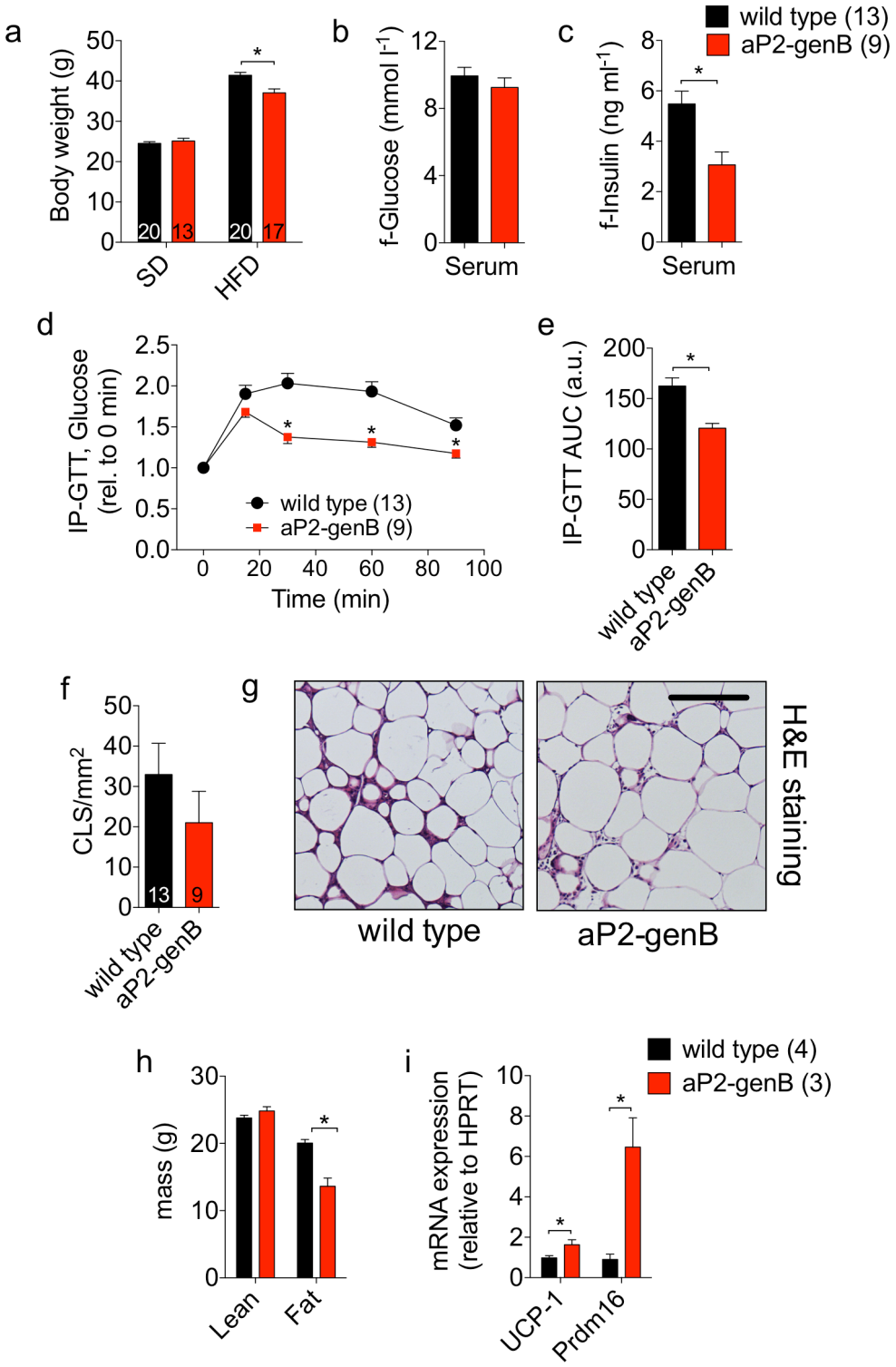

Figure legend on next page

Figure S9. Response to HFD feeding in aP2-genB mice, related to Figure 1. Male aP2-genB and WT littermate mice fed HFD for 10 weeks were used for the experiments. (a) Body weight measurements on standard diet (SD) were done at the age of 8 weeks before the HFD started. Fasting (b) glucose and (c) insulin levels, (d) IP-GTT and (e) AUC analysis. (f) Quantification of crown-like structures from representative images of HE stained eWAT paraffin sections (g). (h) Body mass composition analysis using DEXA. (i) Real time PCR analysis of transcripts of thermogenic genes in iWAT. Number of mice is indicated in the figure. Data are represented as mean ± SEM. * $p < 0.05$, calculated by using the two-tailed unpaired t-test.

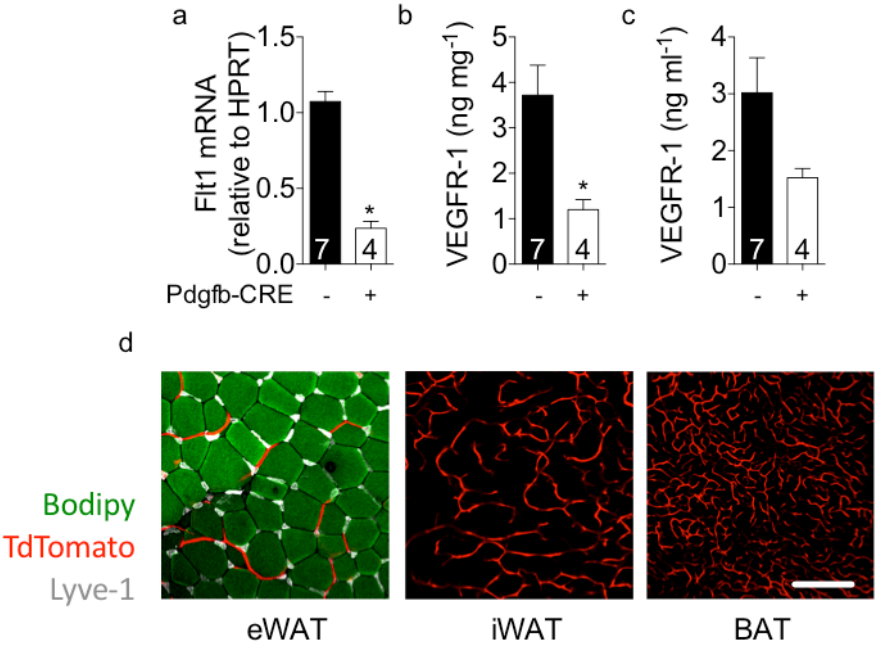

Figure S10. Quantification of the VEGFR1 gene deletion efficiency in endothelial cells, related to Figure 3a and Figure 4. Administration of tamoxifen to adult Flt1$^{fl/fl}$;Pdgfb-CreERT2 mice induced a significant reduction in VEGFR1 (a) mRNA and (b) protein levels in adipose tissue and (c) soluble VEGFR1 protein concentration in serum. (d) Recombination induction by tamoxifen-activated Pdgfb-CreERT2 in endothelial cells of adipose tissue was validated in STOP-lox Rosa26-TdTomato reporter mice. Number of mice is indicated in the figure. Data are represented as mean ± SEM. Scale bar, 100µm. * $p < 0.05$, calculated with two-tailed unpaired ttest.

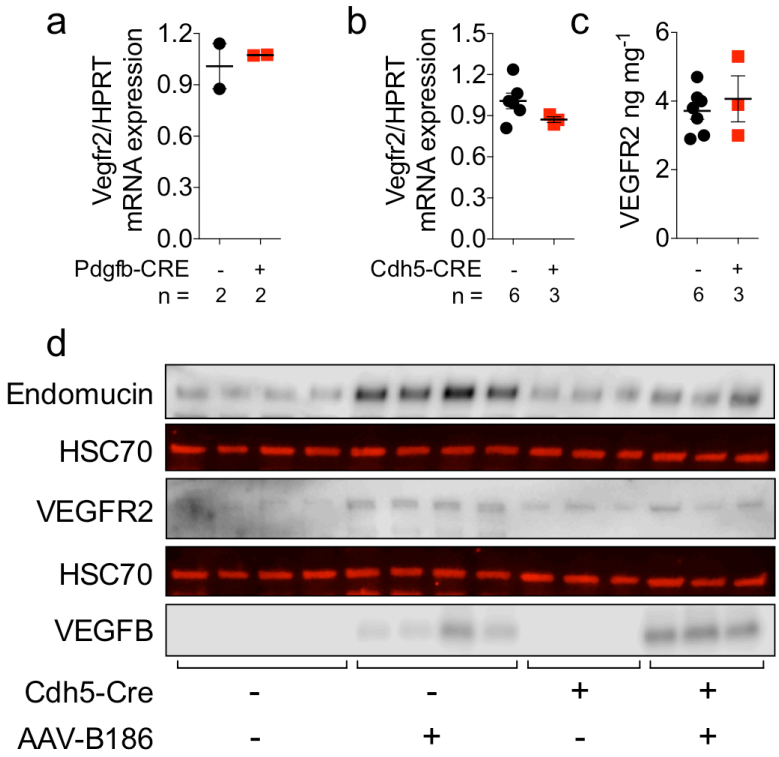

Figure S11. Failure to delete *Vegfr2* in adipose tissue in two mouse models, related to Figure 3. *Vegfr2* deletion was attempted by tamoxifen administration to *Vegfr2*-fl/fl;Pdgfb-CreERT2 male mice or *Vegfr2*-e3fl/e3fl;*Cdh5*(BAC)-CreERT2 female mice. Real time PCR analysis of *Vegfr2* levels in (a) eWAT or (b) iWAT. VEGFR-2 levels analyzed by (c) ELISA (RnD Systems) and (d) Western blot in gonadal WAT. The number of mice is indicated in the figure.

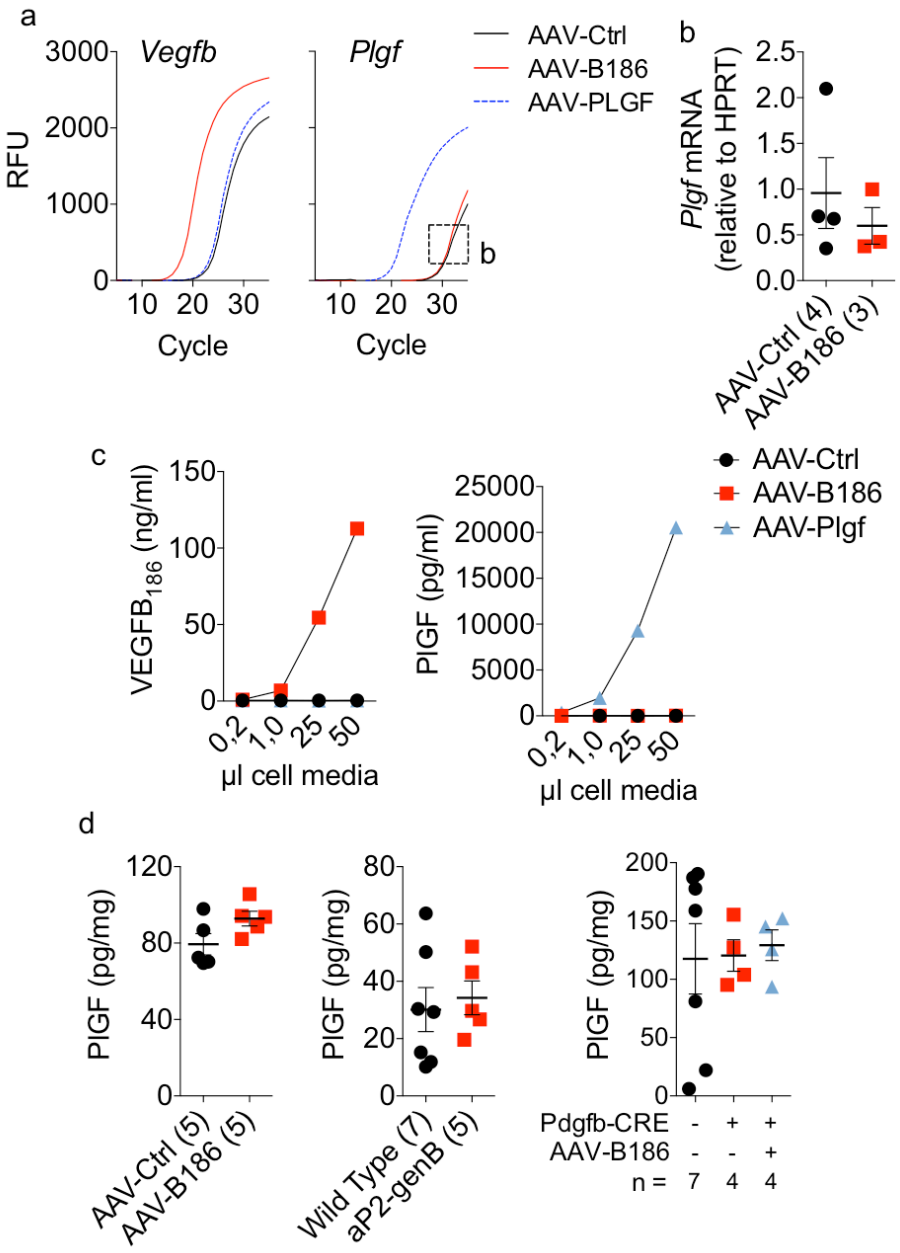

Figure S12. VEGFB did not affect the PLGF expression in adipose tissue, related to Figure 3. (a) Real time PCR amplification curves from mice transduced with the indicated AAVs. (b) Relative *Plgf* mRNA levels normalized to *Hprt* housekeeping gene. (c) $VEGFB_{186}$ and PlGF ELISAs of cell culture media from HEK-293 cells transduced with the indicated AAVs, which demonstrated no cross-reactivity between the two assays. (d) Analysis of PlGF levels in adipose tissue from three different experiments: AAV-transduced wild type, aP2-genB and AAV-transduced Flt1-floxed mice respectively. The number of mice is indicated in the figure.

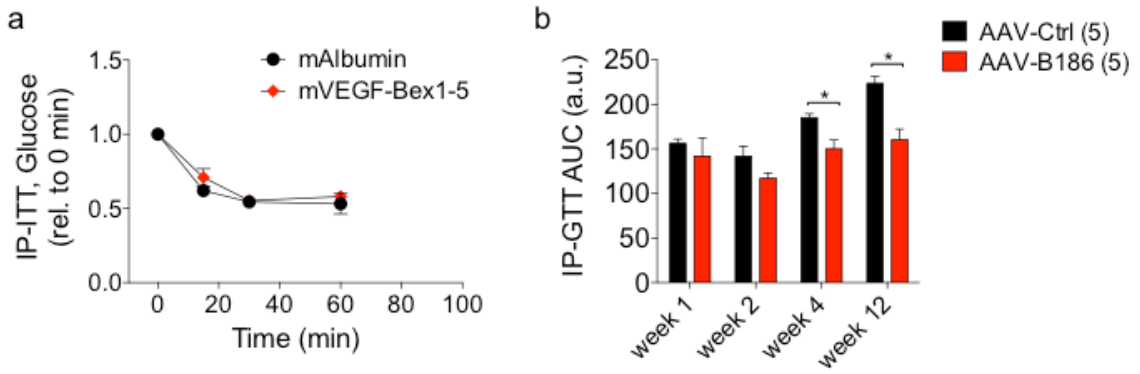

Figure S13. The effect of VEGFB on glucose tolerance requires prolonged exposure, related to Figure 4. C57Bl/6J male mice fed standard diet and treated with the indicated purified proteins or AAVs were used for the experiments. (a) IP-ITT was performed in mice injected i.p. with mouse VEGFBex1-5 or mouse serum albumin at the same time as insulin. (b) Area under the curve from intra-peritoneal glucose tolerance tests performed at indicated time after AAV administration. Number of mice is indicated in the figure. Data are represented as mean ± SEM. * $p < 0.05$, calculated by using the two-tailed unpaired t-test.

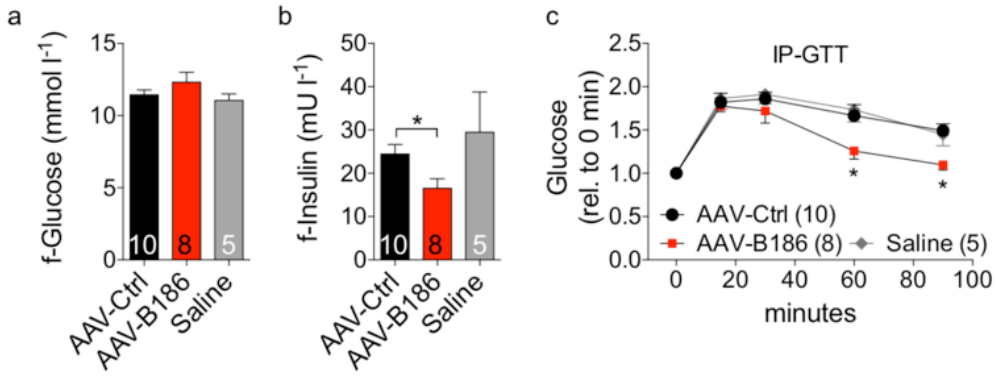

Figure S14. Improved glucose metabolism in apoE*3Leiden;hCETP-Tg mouse model, related to Figure 1 and 4. ApoE*3Leiden;hCETP-Tg males transduced with AAVs and fed HFD were used for the experiments. Saline group was used as and extra control in the experiments. Fasting (a) glucose and (b) insulin levels and (c) intra-peritoneal glucose tolerance test were measured after eight weeks of high fat diet. Number of mice is indicated in the figure. Data are represented as mean ± SEM. * $p<0.05$, calculated with one-way ANOVA, Holm-Sidak's multiple comparisons test.

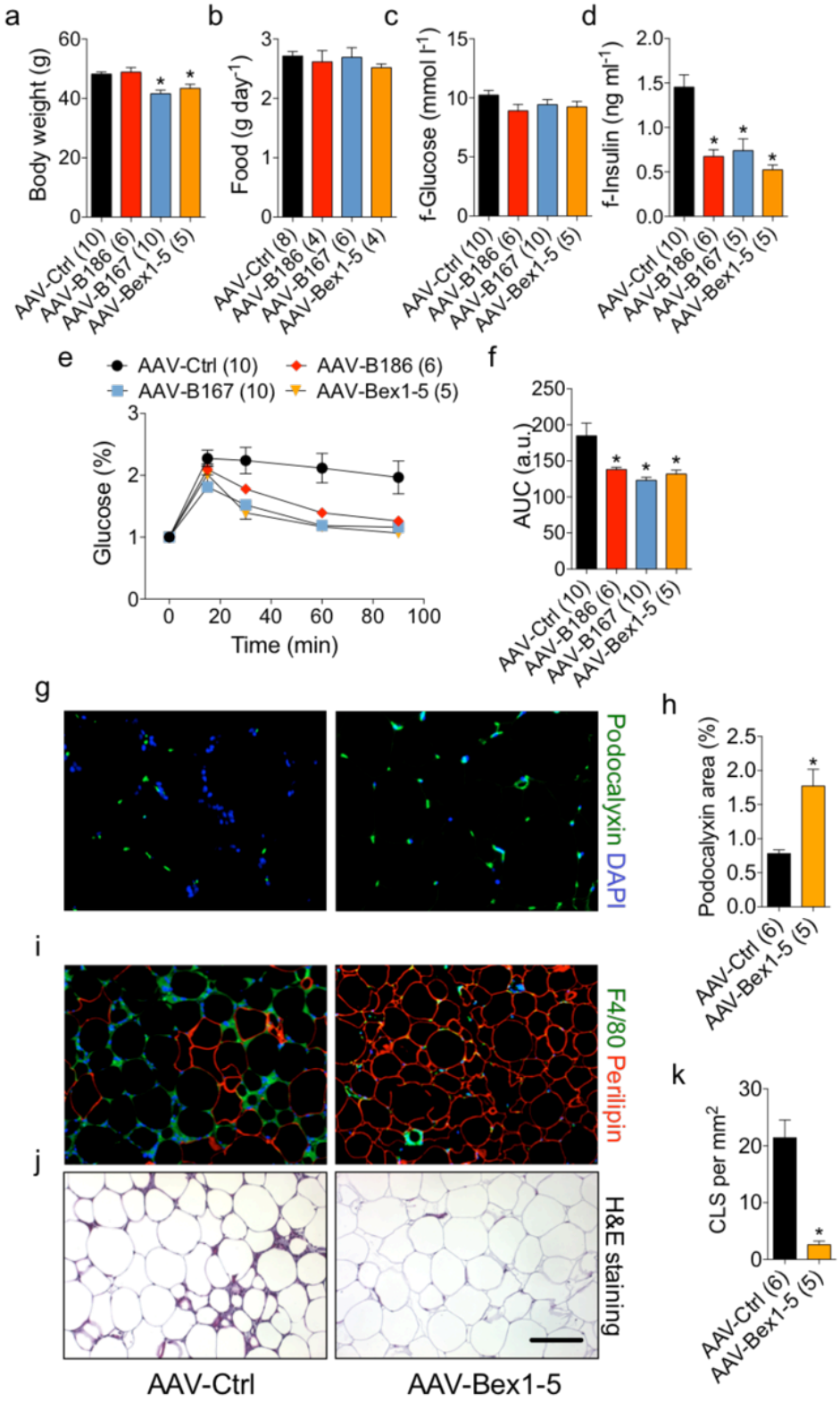

Figure legend on the next page

Figure S15. Response to diet induced obesity in AAV-B186, AAV-B167 and AAV-Bex1-5 mice, related to figure 4. C57Bl/6J male mice transduced with the indicated AAVs and fed HFD for 6 weeks were used for the experiments. (a) Body weight, (b) food consumption, fasting (c) glucose and (d) insulin levels, (e) IP-GTT and (f) AUC analysis are shown. Representative images and quantification of eWAT paraffin sections stained for (g, h) blood vessels or (i-k) crown-like structures. Number of mice is indicated in the figure. Data are represented as mean ± SEM. Scale bar, 100μm. * $p < 0.05$, calculated by using the one-way ANOVA, Holm-Sidak's multiple comparisons test (a-f) or two-tailed unpaired t-test (i-k).

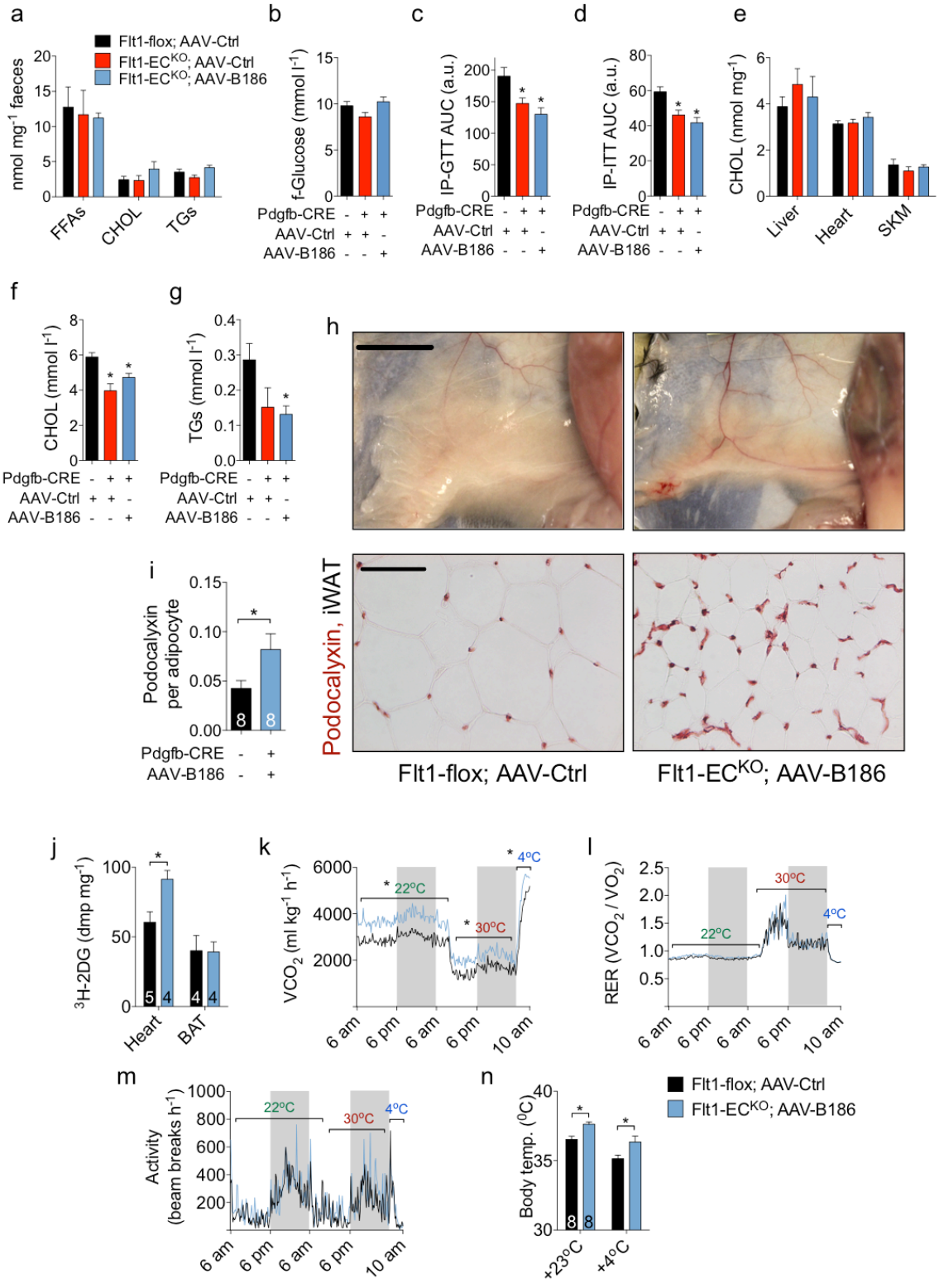

Figure legend on the next page

Figure S16. Detailed characterization of the response to diet induced obesity in Flt1-flox;Pdgfb-CreERT2 (Flt1-EC^{KO}) mice transduced with AAV-B186, related to Figure 5. (a) Lipid analysis from the faeces, (b) fasting levels of blood glucose, AUC from intraperitoneal (c) glucose and (d) insulin tolerance tests. Cholesterol levels in (e) tissues and (f) serum, and (g) fasting triglyceride levels in serum. (h) Macroscopic appearance of inguinal white adipose tissue (iWAT). (i) Paraffin sections from inguinal white adipose tissue (iWAT) were stained for endothelial cell marker podocalyxin. The podocalyxin area was normalized to the number of adipocytes per field to quantify more accurately the changes in vessel density. (j) 2-Deoxy glucose uptake in indicated tissues. (k) Carbon dioxide production rate (l) respiratory exchange ratio and (m) locomotor activity. (n) Body temperature at 23°C ambient temperature and after acute cold exposure at 4°C. Scale bar, 1 cm in h and 50 µm in i. N = 4 – 7 in panels a, e – g, j; n = 6 – 9 mice per group in panels b – d, k-n. Data are represented as mean ± SEM. * $p < 0.05$, calculated by using the one-way ANOVA, Holm-Sidak's multiple comparisons test (a-g) or with two-tailed unpaired ttest (i-n).

Animals

All animal experiments were approved by the Regional State Administrative Agency for Southern Finland.

Mice were housed in individual ventilated cages located in an SPF area with periodical health monitoring and a light cycle from 6 am. The veterinarian of the Laboratory Animal Centre (LAC) of the University of Helsinki monitored the microbiological status of the animal facilities with periodical tests four times a year following FELASA (Federation of European Laboratory Animal Science Associations) guidelines and recommendations (http://www.felasa.eu/document-library/cat_view/17-guidelines-a-recommendations/19-health-monitoring).

Cages were changed once a week and the environment was enriched with plastic hideouts, wooden sticks and nesting material. Temperature in the cages was monitored daily and records showed to be between 22-23^{0}C throughout the year. Humidity dropped to 20% during winter time and increased up to 60% during summer time without a noticeable effect on experimental procedures or weight gain. Mice were fed a standard diet (SD) or a high fat diet (HFD) containing 60% calories from fat (Reseach Diets, D12492). HFD was added in the cages in small portions twice a week and replaced every week.

Wild type C57BL/6JOlaHsd male mice were purchased from Harlan at 5-6 weeks of age and were used in experiments after one week of accommodation period.

Vegfb$^{-/-}$ mice, a kind gift from Dr. Graham F. Kay (Queensland Institute of Medical Research, Australia), were maintained on C57BL/6JCrl (Charles River) background (Bellomo et al., 2000).

Flt1-flox/flox mice were a kind gift from Dr. Napoleone Ferrara (Ambati et al., 2006). Pdgfb-CreERT2 (Claxton et al., 2008), Rosa26-CreERT2 and Vav-Cre mouse line were purchased from The Jackson Laboratory. Flt1-fl/fl;Pdgfb-CreERT2 mice were maintained on C57Bl/6N background. Flt1-fl/fl;Rosa26-CreERT2 and Flt1-fl/fl;Vav-Cre mice were maintained on C57Bl/6J (JAX) background.

Ai9 mice from JAX were used to determine the recombination efficiency and specificity of Pdgfb-CreERT2 mice.

Vegfr2-fl/fl mice (Haigh et al., 2003) were crossed with Pdgfb-CreERT2 (Claxton et al., 2008) mice.

Vegfr2-e3fl/e3fl mice (Hooper et al., 2009) were crossed with *Cdh5*(BAC)-CreERT2 (Okabe et al., 2014), which were both kindly provided by Dr. Yoshiaki Kubota.

Tamoxifen (Sigma-Aldrich) dissolved in corn oil was used administered by oral gavage, 2 mg/100µl/day for 3-4 consecutive days, to 6-8 week old mice.

It is important to note that the C57BL/6JOlaHsd and C57Bl/6N, which were used for the majority of the experiments in this paper, do not have the Nnt1 deletion. This was verified by in house genotyping.

Generation of aP2-genB mice

Mouse *Vegfb* genomic sequence (genB) was inserted after the promoter sequence of aP2 (adipocyte Protein 2, also called fatty acid binding protein 4, FABP4) in a pVK1 vector. Construct was verified by sequencing and validated in vitro where production of both VEGF-B isoforms, 186 and 167, and the response to PPAR gamma activation was observed (data not shown). aP2-genB construct was excised from the plasmid, purified and microinjected in C57BL/6JOlaHsd zygotes. 359 zygotes were injected and transferred to foster mothers. 44 pups were born of which only one pup carried the transgene, the founder mouse. Mating was performed always between one transgenic mouse and one wild type C57BL/6JOlaHsd mouse. Both sexes of transgenic mice were fertile and developed normally but were not borne in a Mendelian ratio.

Adeno-associated viral vector transduction

Adeno-associated viral vectors of serotype 9 (AAV9), encoding a scrambled sequence (AAV-Ctrl) or mouse $Vegfb_{186}$ (AAV-B186) $Vegfb_{167}$ (AAV-B167), $Vegfb_{ex1\text{-}5}$ (AAV-Bex1-5) or $Vegf_{164}$ (AAV-A164) were administered intraperitoneally (i.p.) at doses between 0.4 to 2 x 10^{11} viral particles per mouse. Few initial studies were performed by injections into fat pad but these did not show any differences in expression efficiency, specificity or phenotype when compared with i.p injections.

VEGF/VEGFR-2 blockade

Six-week old wild type C57BL/6JOlaHsd male mice were transduced with AAV-Ctrl or AAV-B186. The two groups, 8 + 8, were split in 2 subgroups with received either injection with vehicle (PBS) or DC101 (0.8 mg per mouse, BioXCell). First injection was performed one day after AAV administration followed by three injections every 3-4 days. Mice were analysed two weeks after transduction with AAVs.

Anesthesia

Ketamine/xylizine injeted i.p. was used as anesthesia for intravenous injections, DEXA measurement or for necropsy. Isoflurane anesthesia was used for intravital imaging.

Body composition

Mice were anesthetised with Ketamine/xylizine injected i.p. and the body composition measurements were performed using Lunar PIXImus Dual-Energy X-ray Absorptiometry (DEXA).

In vivo adipose tissue lipolysis

Inhibition of adipose tissue lipolysis by insulin was assed by quantification of glycerol levels (BioVision Triglyceride Assay, excluding lipase) in serum before and 30 min after insulin injection, 0.75 U/kg administered i.p. Mice were fasted in the morning around 7:00 am and tests were performed in the afternoon around 1:00 pm.

Whole body glucose test

ApoE*3Leiden;hCETP-Tg male mice fed a Western diet (60% calories from fat + 0.25% cholesterol; Research Diets) for 10 weeks were injected i.p. with a trace amount of [U-^{13}C]-glucose (0.1 g/kg) after a 5 h fast. Blood glucose levels were measured before tracer injection and at 10, 20, 30, 40, 50, 60, 75 and 90 minutes thereafter. At the same timepoints, a small drop of blood was collected on filterpaper to measure enrichment of the glucose label using GC/MS. Extraction of glucose from the blood spots, sample derivatization and measurement, as well as calculations were performed as described

previously (van Dijk et al., 2013). These studies were performed at the University of Groningen.

Analysis of whole-body metabolism

Oxygen consumption, carbon dioxide production and locomotor activity were recorded by Oxymax Lab Animal Monitoring System (CLAMS; Columbus Instruments, OH, USA). The mice were kept in individual cages inside a CLAMS chamber for 3 days. After the first day of accommodation mice were monitored for 24 hours at room temperature (+22°C) followed by 20 hours at thermo-neutral temperature (+30°C) and a 4 hours cold exposure (+4°C). Measurements were performed for a total of six Flt1-flox; AAV-Ctrl and six Flt1-EC^{KO}; AAV-B186 mice fed HFD for less than three weeks, before overt differences in body weight were established between the two groups. Energy expenditure was measure calculated using the following formula EE = $(15{,}818*VO_2)+(5{,}176*VCO_2)$ and normalized to lean mass measured by DEXA.

Food consumption

An exact amount of food was added in the food hoppers and was measured after 3-4 days to determine the amount of food consumed per day per animal. Measurements were done with HFD and in few cages the mice crumbled the food excessively and had to be excluded from the measurements. For experiments performed with Flt1-flox mice the measurements were repeated at two different time points during the HFD feeding period from single caged mice. Because of striking differences in body weight observed in Flt1-flox mice we also collected the feces from HFD fed mice to determine the excreted lipids.

Intra-peritoneal glucose and insulin tolerance tests (IP-GTT and IP-ITT)

Mice were fasted for 4-7 hours before the experiments. Food was removed in the morning, mice were placed in new cages to remove possible food from the bedding and tests were performed in afternoon. For intra-peritoneal glucose tolerance test (IP-GTT) 1 g/kg glucose was injected to HFD fed mice and 2 g/kg was injected to SD fed mice. For intra-peritoneal insulin tolerance test (IP-ITT) 0.75 U/kg insulin (Actrapid, Novo Nordisk) was injected to HFD fed mice. 0.5 U/kg insulin was injected to SD fed mice to

determine the effect of acute injection of VEGF-Bex1-5 protein (2.5 μg/mouse) on insulin function. Glucose levels were measured from the tail tip puncture using Contour blood glucose meter (Bayer).

2-Deoxy glucose (2DG) uptake

2DG uptake was determined in conscious and unrestrained mice by i.p. injection of 50 μCi/kg of 2-[1,2-^{3}H(N)]-deoxy-D-glucose together with 0.75 U/kg insulin (Actrapid, Novo Nordisk). Mice were anesthetized after 30 minutes and perfused transcardially with cold PBS before tissue harvesting. Tissues were collected in cold PBS, cut, weighed and solubilized in SOLVABLE (PerkinElmer). Radioactivity was measured from tissue lysates by liquid scintillation using Optiphase HiSafe 3 (Perkin-Elmer) and Wallac LS Counter (Turku, Finland).

Hyperinsulinemic-Euglycemic Clamp (IC)

Catheters were implanted in a carotid artery and a jugular vein of mice for sampling and intravenous infusions 5 days before IC (Ayala et al., 2006). IC (2.5 mU•kg^{-1}•min^{-1}) was performed on 5hr-fasted mice since they have ample glycogen stores and do not undergo the dramatic weight loss seen after an overnight fast (Ayala et al., 2006). [3-^{3}H]glucose was infused to determine glucose flux rates (Berglund et al., 2008). Blood glucose was clamped at ~7.5mmol/L using a variable glucose infusion rate (GIR). Mice received washed erythrocytes from donors to prevent the drop in hematocrit that would otherwise occur from repeated sampling. Euglycemia was achieved by assessment of blood glucose every 10min with GIR adjusted as needed. Blood was taken at 80-120min for the determination of [3-^{3}H]glucose. Clamp insulin was determined at t=100 and 120min. At 120min the clamp was sustained and a 13μCi 2[^{14}C]deoxyglucose ([^{14}C]2DG) bolus was administered intravenously. Blood was taken at 122-155min for [^{14}C]2DG determination. After the last sample, mice were anesthetized and tissues were excised.

Non-esterified fatty acid (NEFA) concentrations were measured by an enzymatic colorimetric assay (NEFA C kit, Wako Chemicals). Plasma and tissue radioactivity of [3-^{3}H]glucose, [^{14}C]2DG, and [^{14}C]2DG-6-phosphate were determined as described (Ayala et al., 2007). Glucose appearance (Ra), endogenous glucose appearance (EndoRa), and

glucose disappearance (Rd) rates were determined using non-steady-state equations (Steele et al., 1956). The glucose metabolic index (Rg) was calculated as described (Kraegen et al., 1985).

Blood collection

Blood was collected from saphenous vein puncture of conscious mice restrained in a tube or from heart puncture in terminally anesthetized mice.

ELISA

ELISA was used to quantify protein levels of mouse insulin (Crystal Chem), human insulin (10-1132-01, Mercodia), mouse VEGFR-1 (DuoSet, DY471, RnD Systems), mouse PLGF (DY465, RnD Systems).

Mouse VEGF-B_{186} was measured by an in house optimized ELISA using capture antibody AF590 (0.8 µg/ml), biotinylated detection antibody BAF767 (0.05 µg/ml) and recombinant mouse VEGF-B_{186} 767-VE (25 ng/ml to 0.04 ng/ml) all from R&D Systems. PBS-0.1%Tween20-1%BSA was used as blocking buffer, PBS-0.1%Tween20-0.1%BSA as dilution buffer and PBS-0.1% Tween20 as washing buffer. This ELISA does not detect VEGF-B_{167}.

Histology

Tissues collected from terminally anesthetized mice were cut and fixed in 4% PFA, ON at $+4^0$C. Adipose tissue was analyzed either as whole mount staining or embedded in paraffin and cut in 5 µm sections. Other tissues were embedded in paraffin or in OCT (Tissue-Tek) after cryoprotection with 25% sucrose using standard protocols. Heart and skeletal muscle were freshly embedded in OCT.

Hematoxylin-eosin stainings were used for basic histological assessment.

Immunohistochemistry on paraffin and cryosections was performed after standard protocols using TNT wash Buffer and TNB Blocking Buffer (PerkinElmer). For whole mount IHC tissues were washed and permeabilized using PBS, 0.3% Tx100 and blocked with donkey immunomix (5% normal donkey serum, 0.2% BSA, 0.3% Triton-X 100 and 0.05% NaN_3).

The following primary antibodies were used for immunostaining of mouse tissues diluted in TNB or donkey immunomix: rat anti PECAM-1 (diluted 1:500; clone MEC 13.3, 553370, BD Biosciences), hamster anti PECAM-1 (diluted 1:500; clone 2H8, MAB1398Z, Chemicon), rabbit anti NG2 (diluted 1:500; AB5320, Millipore), polyclonal goat anti mouse VEGFR-3 (diluted 1:100; AF743, R&D Systems), guinea pig anti Perilipin (Diluted 1:2500, 20R-PP004, Fitzgerald), guinea pig anti Perilipin 5 (diluted 1:200, GP31, Progen), rabbit anti-UCP1 antibody (1:200, ab10983), rat anti mouse F4/80 (diluted 1:500, BD Biosciences), mouse anti glutamine synthethase (diluted 1: 200, BD Biosciences) and mouse anti Cyp1a2 (diluted 1:100, sc-53241, Santa Cruz).

For immunofluorescense the appropriate secondary antibody conjugated with Alexa Fluor 488, Alexa Fluor 594, Alexa Fluor 633 or Alexa Fluor 647 were used (diluted 1:500; Molecular Probes/Invitrogen). For immunohistochemistry on sections the appropriate biotinilated antibodies (diluted 1:300, VectorLabs) were used followed by two rounds of amplification using a TSA kit (PerkinElmer). AEC (SigmaAldrich) was used as chromogen.

Immunofluorescence images were taken with a Zeiss LSM780 confocal microscope, Zeiss Axioplan 2 or Zeiss Axio Imager widefield epifluorescense microscopes. Bright-field sections were imaged with a Leica DM LB microscope (Leica Microsystems) equipped with an Olympus DP50 color camera (Olympus Soft Imaging Solutions GMBH) or with 3DHISTECH Pannoramic 250 FLASH II digital slide scanner at Genome Biology Unit (Research Programs Unit, Faculty of Medicine, University of Helsinki, Biocenter Finland). Image analysis was carried out using the ImageJ software (NIH).

Vessel perfusion and leakage

C57BL/6JOlaHsd male mice were transduced with AAVs for four weeks or more. Tail vein or retro-orbital injection were performed to mice under ketamine/zylazine anesthesia. FITC, DyLight-488 or DyLight-594 Labeled Lycopersicon Esculentum (Tomato) Lectin (50µg/100µl/mouse, VecorLabs) were used to determine microvasculature perfusion. Adipose tissue was excised, fixed in PFA, counterstained and imaged as described for whole mount staining.

Vessel leakage was analyzed by retro-orbital injection of FluoSpheres® Carboxylate-Modified Microspheres, 0.1 µm, 580/605 (100µl per mouse, 0.4% suspension in PBS, Molecular Probes/Invitrogen). Capillaries were counterstained with DyLight-488 Tomato Lectin (50µg/100µl/mouse, VecorLabs). Mice were perfused transcardially with PBS to remove the excess of FluoSpheres in the lumen followed by perfusion-fixation with 2% PFA and imaging with confocal. High magnification optical sections were acquired to determine if the few microspheres that were left in the capillaries were inside or outside of the lumen.

Intravital two-photon microscopy and blood flow measurement

C57BL/6JOlaHsd male mice were transduced with AAVs for six weeks or more. Animals were anesthetized with isoflurane (4.0%−induction, 2.2%-1.2%−maintenance) using Univentor 410 gas anesthesia unit. During preparation and imaging animals respiration rate (RR), heart rate (HR) and body temperature were monitored and kept stable (RR=50±10 and HR=480±50 with PhysioSuite (Kent Scientific) pulse oximeter, 37 ^{o}C with TMP-5b heating pad, Supertech). eWAT was exposed through the small incision and attached with Loctite-401 cyanoacrylate glue to a custom-made metal holder, which was then mounted to the microscope stage. Texas Red 70 KDa dextran conjugate (D1830, Molecular Probes) was injected intravenously (50-60 µl of 1% solution in physiological saline) for blood plasma visualization. Imaging was done with Zeiss AxioExaminer LSM7 MP microscope equipped with Coherent Chameleon Vision mode-locked tunable laser and Zeiss W Plan-Apochromat 20X/1.0 objective. Following parameters were used for image acquisition: excitation wavelength set to 860 nm, emission bandpass filters: 500-550 nm for BODIPY and 601-657 nm for Texas Red, pixel dwell time 1.3 µs, laser power at 3%-20% depending on the depth of imaging. Blood flow was measured with line scans at 0.003-0.01 Hz repetition rate as previously described (Helmchen and Kleinfeld, 2008).

Lipid analysis

For tissue lipid analysis a scaled down Bligh & Dyer extraction method was used. Wet tissue or dried feces (10 – 50 mg) were homogenized in 0.5 ml $CHCl_3$:MeOH (2:1) using

Ceramic Beads Tubes (Cat # 13113-50, Mo Bio). Lysate and beads were transfered in 15 ml conical tubes (Greiner bio-one # 188271) and mixed with 1 ml $CHCL_3$ and 1.5 ml 0.9% NaCl to create the aqueous and organic phase. The organic phase was collected with a Pasteur pipet, transferred in 2 ml Eppis and evaporated in a SpeedVac. Lipids were re-suspended in PBS - 5% Tx100, at 95^0C with continuous mixing for 20-30 min. Cholesterol and triacylglycerol concentrations were determined with enzymatic methods (Roche Diagnostics Hitachi). Free fatty acid levels were measured with NEFA R2 kit downscaled to microplate format (Wako).

For mass spectrometry hepatic total lipids were extracted according to Folch et al. (Folch et al., 1957). The sample solutions in chloroform/methanol (1:2, v/v) were spiked with a cocktail of 14 internal standards and supplemented with 1% NH_4OH just before infusion into a triple quadrupole mass spectrometer (Agilent 6490 Triple Quadr LC/MS with iFunnel technology, California, USA). The diverse lipids were detected in the positive or negative ionization mode and using class-specific detection modes when applicable (Brugger et al., 1997; Duffin et al., 1991; Sullards and Merrill, 2001). First the individual lipid species were identified and quantified as detailed previously (Haimi et al., 2006; Kakela et al., 2003), and then the lipid class concentrations were calculated as the sum of all individual species of the class.

Real-time PCR

Total RNA was isolated from tissue using TRIsure reagent (Bioline, Luckenwalde, Germany) and further purified with NucleoSpin RNA II (Macherey-Nagel). RNA was transcribed to cDNA using iScript kit (Bio-Rad) and qPCR was carried out following standard procedures using SYBR green or TaqMan primer-probe sets. All data were normalized to 36B4, HPRT or GAPDH housekeeping genes, and quantification was performed using the $2^{-\Delta\Delta CT}$ method.

Primers sequences are as follows:

HPRT,

fwd. TTGCTCGAGATGTCATGAAGGA,

rev. AGCAGGTCAGCAAAGAACTTATAG;

36B4,

fwd. GGACCCGAGAAGACCTCCTT,
rev. GCACATCACTCAGAATTTCAATGG.
VEGF-B,
fwd. AGCCACCAGAAGAAAGTGGT,
rev. GCTGGGCACTAGTTGTTTGA;
Flt1,
fwd. TTGAGGAGCTTTCACCGAAC,
rev. GGAGGAGTACAACACCACGG;
F4/80,
fwd. CCAGGCTTTGTCTTGAATGG,
rev. TAGCTTCCGAGAGTGTTGTG;
TNFalpha,
fwd. CCCTCACACTCAGATCATCTTCT,
rev. GCTACGACGTGGGCTACAG;
IL-6,
fwd. CCAGTTGCCTTCTTGGGACT,
rev. GGTCTGTTGGGAGTGGTATCC;
MCP-1,
fwd. ACTGAAGCCAGCTCTCTCTTCCTC,
rev. TTCCTTCTTGGGGTCAGCACAGAC;
IL-1beta,
fwd. CTGGTGTGTGACGTTCCCATTA,
rev. CCGACAGCACGAGGCTTT;
iNOS,
fwd. CAGAGGACCCAGAGACAAGC,
rev. TGCTGAAACATTTCCTGTGC;
ARG-1,
fwd. CTCCAAGCCAAAGTCCTTAGAG,
rev. AGGAGCTGTCATTAGGGACATC,
IL-10,
fwd. GCTCTTACTGACTGGCATGAG,

rev. CGCAGCTCTAGGAGCATGTG;
TGFbeta1,
fwd. AAGTTGGCATGGTAGCCCTT,
rev. GCCCTGGATACCAACTATTGC;
PRDM16,
fwd. CAGCACGGTGAAGCCATTC,
rev. GCGTGCATCCGCTTGTG;
UCP-1,
fwd. CTTTGCCTCACTCAGGATTGG,
rev. ACTGCCACACCTCCAGTCATT;
Cidea,
fwd. TGACATTCATGGGATTGCAGAC
rev. GGCCAGTTGTGATGACTAAGAC
TaqMan probes were used for GAPDH (4352932E), PECAM1/CD31 (Mm01246167_m1).

Western blotting and immunoprecipitation

A standard PAGE protocol was used to separate the proteins under reducing conditions. High fat containing tissues were centrifuged 3-4 times to remove the excess fat, which prevents proper separation of protein. For VEGF-B immunoprecipitation, 100 ul serum was diluted with 400 ul PBS and incubated with 3 µl hVEGF-R1-Fc (1 µg/ul) for 2 h at 4°C on a rotary mixer. 50 ul of 50% protein G sepharose suspention was added and the mixture was further incubated o/n at 4°C on a rotary mixer. The immunoprecipitate was separated by centrifugation at 3500 rpm 2 minutes (bench top centrifuge) and washed for 3 x 10 minutes with PBS-T 0,05%. Then the immunoprecipitate was solubilized in 2x Laemli buffer by boiling for 5 minutes at 95°C, centrifuged for 3 min at 14000 rpm and the clear supernatant was resolved in reducing PAGE. Westernblot bands were quantified using ImageJ or Image Studio Lite (LI-COR).

Antibodies used for westernbloting were: mouse anti mouse Hsc70 (sc-7298, SantaCruz), rabbit anti mouse rpS6 (Cell Signaling), goat anti mouse VEGF-B 167/186 (AF590, R&D

Systems), rabbit anti mouse Akt and P-AKT Ser473 (Cell Signaling) and goat anti Podocalyxin (AF1556, R&D Systems).

Statistics

The results are shown as means ± SEM. All statistical analyses were performed by two-tailed unpaired t-test for two-group comparisons (or a paired t-test were appropriate) and one-way ANOVA for multiple groups (GraphPad, Prism). A p-value less than 0.05 was considered significant.

Supplementary references

Ambati, B.K., Nozaki, M., Singh, N., Takeda, A., Jani, P.D., Suthar, T., Albuquerque, R.J., Richter, E., Sakurai, E., Newcomb, M.T., et al. (2006). Corneal avascularity is due to soluble VEGF receptor-1. Nature *443*, 993-997.

Ayala, J.E., Bracy, D.P., Julien, B.M., Rottman, J.N., Fueger, P.T., and Wasserman, D.H. (2007). Chronic treatment with sildenafil improves energy balance and insulin action in high fat-fed conscious mice. Diabetes *56*, 1025-1033.

Ayala, J.E., Bracy, D.P., McGuinness, O.P., and Wasserman, D.H. (2006). Considerations in the design of hyperinsulinemic-euglycemic clamps in the conscious mouse. Diabetes *55*, 390-397.

Bellomo, D., Headrick, J.P., Silins, G.U., Paterson, C.A., Thomas, P.S., Gartside, M., Mould, A., Cahill, M.M., Tonks, I.D., Grimmond, S.M., et al. (2000). Mice lacking the vascular endothelial growth factor-B gene (Vegfb) have smaller hearts, dysfunctional coronary vasculature, and impaired recovery from cardiac ischemia. Circulation research *86*, E29-35.

Berglund, E.D., Li, C.Y., Poffenberger, G., Ayala, J.E., Fueger, P.T., Willis, S.E., Jewell, M.M., Powers, A.C., and Wasserman, D.H. (2008). Glucose metabolism in vivo in four commonly used inbred mouse strains. Diabetes *57*, 1790-1799.

Brugger, B., Erben, G., Sandhoff, R., Wieland, F.T., and Lehmann, W.D. (1997). Quantitative analysis of biological membrane lipids at the low picomole level by nano-electrospray ionization tandem mass spectrometry. Proceedings of the National Academy of Sciences of the United States of America *94*, 2339-2344.

Claxton, S., Kostourou, V., Jadeja, S., Chambon, P., Hodivala-Dilke, K., and Fruttiger, M. (2008). Efficient, inducible Cre-recombinase activation in vascular endothelium. Genesis *46*, 74-80.

Duffin, K.L., Henion, J.D., and Shieh, J.J. (1991). Electrospray and tandem mass spectrometric characterization of acylglycerol mixtures that are dissolved in nonpolar solvents. Anal Chem *63*, 1781-1788.

Folch, J., Lees, M., and Sloane Stanley, G.H. (1957). A simple method for the isolation and purification of total lipides from animal tissues. The Journal of biological chemistry *226*, 497-509.

Haigh, J.J., Morelli, P.I., Gerhardt, H., Haigh, K., Tsien, J., Damert, A., Miquerol, L., Muhlner, U., Klein, R., Ferrara, N., et al. (2003). Cortical and retinal defects caused by dosage-dependent reductions in VEGF-A paracrine signaling. Dev Biol *262*, 225-241.

Haimi, P., Uphoff, A., Hermansson, M., and Somerharju, P. (2006). Software tools for analysis of mass spectrometric lipidome data. Anal Chem *78*, 8324-8331.

Helmchen, F., and Kleinfeld, D. (2008). Chapter 10. In vivo measurements of blood flow and glial cell function with two-photon laser-scanning microscopy. Methods Enzymol *444*, 231-254.

Hooper, A.T., Butler, J.M., Nolan, D.J., Kranz, A., Iida, K., Kobayashi, M., Kopp, H.G., Shido, K., Petit, I., Yanger, K., et al. (2009). Engraftment and reconstitution of hematopoiesis is dependent on VEGFR2-mediated regeneration of sinusoidal endothelial cells. Cell Stem Cell *4*, 263-274.

Kakela, R., Somerharju, P., and Tyynela, J. (2003). Analysis of phospholipid molecular species in brains from patients with infantile and juvenile neuronal-ceroid lipofuscinosis using liquid chromatography-electrospray ionization mass spectrometry. J Neurochem *84*, 1051-1065.

Kraegen, E.W., James, D.E., Jenkins, A.B., and Chisholm, D.J. (1985). Dose-response curves for in vivo insulin sensitivity in individual tissues in rats. Am J Physiol *248*, E353-362.

Okabe, K., Kobayashi, S., Yamada, T., Kurihara, T., Tai-Nagara, I., Miyamoto, T., Mukouyama, Y.S., Sato, T.N., Suda, T., Ema, M., et al. (2014). Neurons limit angiogenesis by titrating VEGF in retina. Cell *159*, 584-596.

Steele, R., Wall, J.S., De Bodo, R.C., and Altszuler, N. (1956). Measurement of size and turnover rate of body glucose pool by the isotope dilution method. Am J Physiol *187*, 15-24.

Sullards, M.C., and Merrill, A.H., Jr. (2001). Analysis of sphingosine 1-phosphate, ceramides, and other bioactive sphingolipids by high-performance liquid chromatography-tandem mass spectrometry. Sci STKE *2001*, pl1.

van Dijk, T.H., Laskewitz, A.J., Grefhorst, A., Boer, T.S., Bloks, V.W., Kuipers, F., Groen, A.K., and Reijngoud, D.J. (2013). A novel approach to monitor glucose metabolism using stable isotopically labelled glucose in longitudinal studies in mice. Lab Anim *47*, 79-88.